ASCA Observations of the Young Rotation-powered Pulsars PSR B1046−58 and PSR B1610−50

Michael Pivovaroff and Victoria Kaspi
Department of Physics and Center for Space Research, Massachusetts Institute of Technology

and

Eric Gotthelf
Columbia Astrophysics Laboratory, Columbia University

ABSTRACT

X-ray observations of synchrotron nebulae around radio pulsars permit the study of the evolution and basic physical processes of rotation-powered neutron stars. We present *ASCA* GIS and SIS observations of the young pulsars PSRs B1046−58 and B1610−50. Significant non-pulsed emission is detected from the direction of PSR B1046−58. We argue that the emission originates from a synchrotron nebula powered by the pulsar and that the nebula is spatially unresolved by *ASCA*. We have also examined the 99% confidence error region of the previously unknown γ-ray source 3EG J1048−5840, which lies within the GIS FOV. One of two hard sources within the ellipse is coincident with the pulsar. When taken with the γ-ray pulsations from 3EG J1048−5840 reported by Kaspi et al. (1999), this suggests PSR B1046−58 is the eighth known radio pulsar to exhibit γ-rays.

X-ray emission from PSR B1610−50 is not detected. We derive a flux limit and use it show that the pulsar's velocity is unlikely to be greater than ~100 km s^{-1}, casting doubt on a previously reported association between PSR B1610−50 and the supernova remnant Kes 32. Kes 32 is detected, as is evident from the correlation between X-ray and radio emission.

The point-like emission from PSR B1046−58 and the non-detection of PSR B1610−50 contradict previous reports of very large (tens of arc-minutes) nebulae surrounding these pulsars.

1. Introduction

In general, only a small fraction ($10^{-7} - 10^{-5}$) of a rotation-powered pulsar's spin-down luminosity ($\dot{E} \equiv 4\pi^2 I\dot{P}P^{-3}$) manifests itself as radio pulsations. It is believed that a significant fraction of the luminosity emerges as a relativistic wind of positrons and electrons. When this wind is confined by the surrounding medium, an X-ray observable synchrotron nebula results. Measurements of the luminosity, morphology, and spectrum of the synchrotron nebula are essential for determining fundamental properties of the wind, ambient density, and nebular formation mechanisms.

Observations of these two young pulsars, combined with a growing list of other well-studied similarly aged ($\tau_c \equiv P/2\dot{P} \sim 10^3 - 10^5$ yr) and energetic ($\dot{E} \sim 10^{35} - 10^{37}$ ergs s^{-1}) pulsars, allow the study of the population as a whole and promises to help constrain the evolutionary cycle of rotation-powered neutron stars (see e.g. Seward & Wang 1998 and Becker & Trümper 1997). Here we summarize analysis of archival *ASCA* data. This work is discussed in more detail by Pivovaroff, Kaspi, & Gotthelf (1999).

2. Observations and Analysis

ASCA (Tanaka, Inoue, & Holt 1994) observed PSR B1046−58 on 1994 January 27 and PSR B1610−50 on 1994 March 25. We present an analysis of the data obtained from the public archive. For both observations, data were taken with all four imaging spectrometers, each in the focal plane of its own foil mirror: two Solid State Imaging Spectrometers (SIS-0, SIS-1) employing charge coupled devices (CCDs), and two Gas Imaging Spectrometers (GIS-2, GIS-3) employing gas scintillation proportional counters. After filtering the data using standard screening criteria, the resulting effective observation times per single detector are 18 ks (GIS) and 15 ks (SIS) for PSR B1046−58, and 11 ks (GIS) and 8.4 ks (SIS) for PSR B1610−50.

2.1. PSR B1046−58

The flat-fielded GIS image (Figure 1a) contains an oval region of emission whose southern tip is coincident with the radio position, determined by radio interferometric measurements made by Stappers et. al (1999). The GIS FOV also contains the 95% and 99% error ellipse for the unidentified EGRET γ-ray source 3EG J1048−5840. The SIS (Figures 1b−1d) resolves the emission into three distinct sources coincident with a region of apparently diffuse emission. The proximity of the sources and the possibly diffuse emission complicates calculation of the detection significance for each source. All three sources (hereafter Src 1, Src 2, & Src 3) have a detection significance of at least 4σ in the SIS. Low statistics prevents detailed spectral studies. Src 1 and Src 3 are distinctly hard (E $>$ 2 keV; see Figure 1d) while Src 2 is distinctly soft (E $<$ 2 keV; see Figure 1c).

Arrival times of GIS events selected from a $4'$ diameter aperture centered on Src 1 were barycentered and folded at an ephemeris calculated from radio timing obtained at the 64-meter radio telescope at Parkes, Australia. No pulsations were found. The upper limit on the pulsed fraction for a sinusoidal pulse shape is 31%. The absence of pulsations from the GIS data is in agreement with the work of Saito (1998).

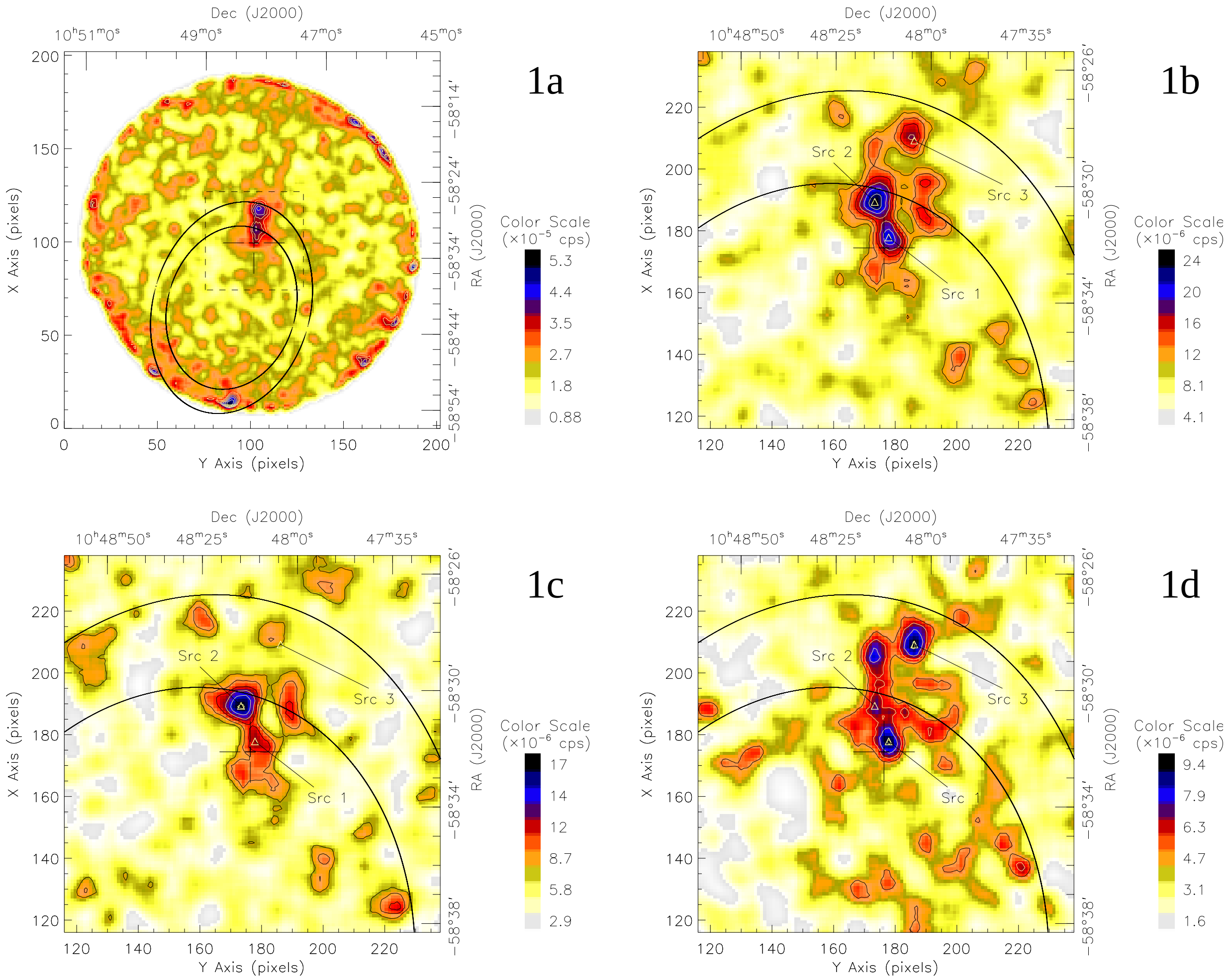

Fig 1.– *ASCA* images of the PSR B1046−58 field: flat-fielded images of the region around the pulsar, whose location is marked by the cross. a) The broad band (0.8−12 keV) GIS image shows an oval shaped region of X-ray emission with the pulsar located at its southern tip. The two ellipses represent the 95% and 99% error regions for the γ-ray source 3EG J1048−5840. The dashed square delineates the SIS region displayed in b)−d). b) The broad band (0.4−10 keV) SIS image clearly showing the three labeled sources embedded in a diffuse emission region. c) The soft band SIS image (0.4−2.0 keV) revealing the soft, probably thermal nature of Src 2. Note that Srcs 1 and 3 are very weak in this band. d) The hard band (2−10 keV) SIS image showing the hard, probably non-thermal nature of Src 1 and Src 3. We identify Src 1, offset 21″ from the radio position of PSR B1046−58 and the only source inside the 95% error circle of the pulsed γ-ray source 3EG J1048−5840, as the synchrotron nebula of PSR B1046−58. Contours approximately correspond to the 4σ, 5σ, 6σ, 7σ, 8σ, and 9σ levels.

Src 1 lies 21″ from the radio position of PSR B1610−50. Taken with the lack of pulsations and the hard (probably) non-thermal spectrum, we identify Src 1 as a synchrotron nebula powered by the pulsar. Using a canonical power law model with photon index two (see e.g. Seward & Wang 1988 or Becker & Trümper 1997) and assuming a column density of $N_H = 5 \times 10^{21}$ cm^{-2}, we derive a $2 - 10$ keV unabsorbed flux $F_x = (2.5 \pm 0.3) \times 10^{-13}$ ergs cm^{-2} s^{-1}. For a pulsar distance of 3.0 kpc, the *ASCA*-band $(2 - 10$ keV) luminosity is $L_x = (2.7 \pm 0.3) \times 10^{32}$ ergs s^{-1}. The conversion efficiency ϵ of spin-down luminosity ($\dot{E} = 2.0 \times 10^{36}$ ergs $^{-1}$) into *ASCA*-band emission is $\epsilon = (1.3 \pm 0.1) \times 10^{-4}$.

2.2. PSR B1610−50

No emission from the direction of the pulsar is detected (see Figures 2a and 2b). Using an extraction aperture centered on the radio position, determined from radio interferometric measurements by Stappers et al. (1999), the combined GIS+SIS data have a detection significance below 2σ. The primarily soft flux in the southeast quadrant of the GIS FOV is scattered emission from the nearby supernova remnant RCW 103. As reported by Kawai, Tamura, & Saito (1998), *ASCA* provides the first X-ray detection of the supernova remnant Kes 32. The emission generally traces the radio morphology. Assuming a canonical power law spectrum and a column density of $N_H = 2{\times}10^{22}$ cm^{-2} gives an unabsorbed $2{-}10$ keV upper flux limit $F_x < 1.5{\times}10^{-13}$ ergs cm^{-2} s^{-1}. For a pulsar distance of 7.3 kpc, the *ASCA*-band luminosity is $L_x < 9.6 \times 10^{32}$ ergs s^{-1}. The conversion efficiency ϵ of spin-down luminosity ($\dot{E} = 1.6 \times 10^{36}$ ergs $^{-1}$) into *ASCA*-band emission is $\epsilon < 6.1 \times 10^{-4}$.

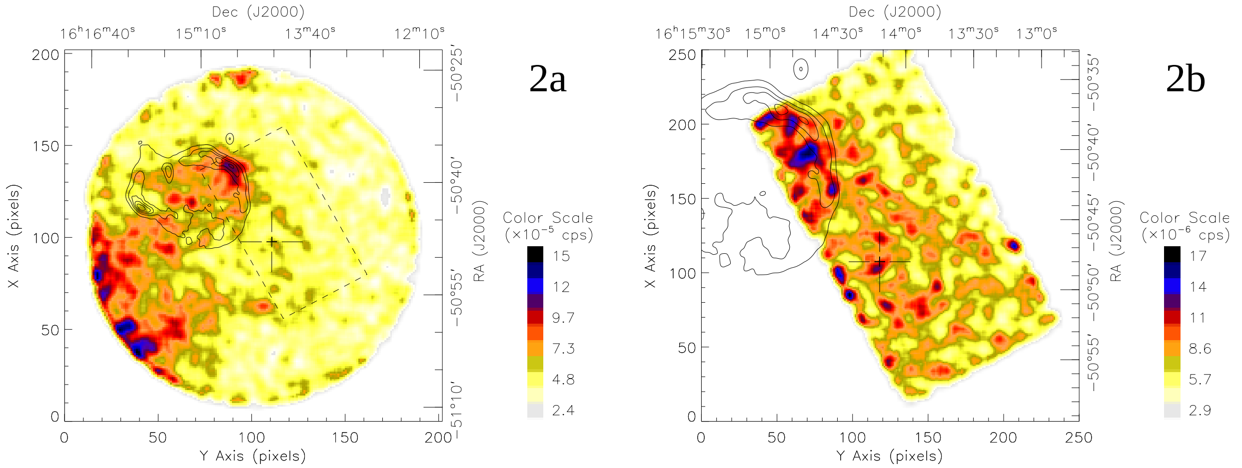

Fig. 2– *ASCA* images of the PSR B1610−50 field: flat-fielded images of the region around the pulsar, whose location is marked by the cross. The dashed rectangle represents the SIS FOV, and the contours, corresponding to 0.04, 0.18, 0.31, 0.44, 0.57, and 0.70 Jy beam^{-1}, are from 843 MHz MOST observations of the supernova remnant Kes 32. a) The broad band (1−10 keV) GIS image. Scattered emission from the nearby supernova remnant RCW 103 is responsible for the large flux gradient that begins in the southeast FOV and extends to the edge of the SIS FOV. b) The hard band (2−10 keV) SIS image shows the correspondence between the radio contours and X-ray emission and the lack of emission from PSR B1610−50.

3. Discussion

The importance of the detection of weak emission from PSR B1046−58 and the non-detection of PSR B1610−50 is most readily understandable in the context of the growing body of work on the X-ray properties of young ($\tau_c < 10^5$ yr) rotation-powered neutron stars. Synchrotron nebula are present around many young pulsars, e.g. Vela, PSR B1706−44, PSR B1509−58 (Harnden et al. 1985, Finley et al. 1998, Seward & Harnden 1982). The hard SIS source (Src 1), offset $21''$ from the radio position is likely to be a synchrotron nebula powered by PSR B1046−58.

Using the luminosity upper limit for PSR B1610−50 and following the prescription of Gotthelf & Kaspi (1998), we constrain the pulsar's velocity to be less than $\sim$100 km s^{-1}, assuming that the pulsar has wind properties similar to other young, Crab-like pulsars. The velocity required by the association of PSR B1610−50 with the supernova remnant Kes 32 proposed by Caraveo (1993) exceeds this upper limit by at least a factor of 20, arguing against the association.

The derived luminosity for PSR B1046−58 and the upper limit for PSR B1610−50 are considerably lower (factors of $\sim 5 - 10$) than those predicted by the empirical $L_x - \dot{E}$ relationships of Seward & Wang (1988) and Becker & Trümper (1997). Distance estimates from the Taylor & Cordes (1993) DM-distance relatinoship are uncertain to 25−50% and can at most increase L_x by a factor of $\sim$3. The discrepancy is not surprising given the many factors apart from $\dot{E}$ that influence the emission mechanisms, such as the pulsar's velocity or the ISM conditions in the vicinity of the neutron star.

The detection of a spatially unresolved ($< 2'$) synchrotron nebula powered by PSR B1046−58 and the lack of emission from PSR B1610−50 contradict previous reports by Kawai et al. (1998) of large ($\sim$tens of arc-minutes) nebulae associated with these young, energetic pulsars.

Acknowledgements

M. Pivovaroff thanks the organizing committee for their financial support in helping him to participate in the first XMM workshop. We thank Bryan Gaensler for providing the radio images of the PSR B1046−58 and PSR B1610−50/Kes 32 fields and for useful discussion. We thank M. Bailes, R. Manchester, and R. Pace for acquiring radio timing data for PSR B1046−58 at the 64-m Parkes radio telescope in New South Wales, Australia. We thank B. Hartman for providing information on 3EG J1048−5840 prior to publication. We have used the NASA maintained HEASARC web site extensively for archival data retrieval and subsequent analysis. M. Pivovaroff is supported in part by NASA under Contract NASA-37716.

REFERENCES

Becker, W. & Trümper, J. 1997, Astr. Astrophys., 326, 682

Caraveo, P. A. 1993, Astrophys. J. Lett., 415, L111

Finley, J. P., Srinivasan, R., Saito, Y., Hiriyama, M., Kamae, T., & Yoshida, K. 1998, Astrophys. J., 493, 884

Gotthelf, E. V. & Kaspi, V. M. 1998, Astrophys. J. Lett., 497, L29

Harnden, F. R., Grant, P. D., Seward, F. D., & Kahn, S. M. 1985, Astrophys. J., 299, 828

Kaspi, V. M., Lackey, J., Mattox, J., Manchester, R. N., & Bailes, M. 1999, Astrophys. J. in preparation

Kawai, N., Tamura, K., & Saito, Y. 1998, Adv. Space Res., 21, 213

Pivovaroff, M., Kaspi, V. M., & Gotthelf, E. V. 1999, Astrophys. J. submitted

Saito, Y. 1998. PhD thesis, University of Tokyo

Seward, F. D. & Harnden, F. R. 1982, Astrophys. J. Lett., 256, L45

Seward, F. D. & Wang, Z.-U. 1988, Astrophys. J., 332, 199

Stappers, B. W., Gaensler, B. M., Johnston, S., & Frail, D. A. 1999. in preparation

Tanaka, Y., Inoue, H., & Holt, S. S. 1994, Proc. Astr. Soc. Jap., 46, L37

Taylor, J. H. & Cordes, J. M. 1993, Astrophys. J., 411, 674

This preprint was prepared with the AAS LaTeX macros v3.0.